Supporting information

Highly stretchable, transparent and conductive double-network ionic hydrogel for strain and pressure sensors with ultrahigh sensitivity

Jie Yu[a], Ming Wang[a], Chao Dang[a], Cunzhi Zhang[a], Xiao Feng[a], Guixian Chen[a], Zhongyuan Huang[a], Haisong Qi[a], Hongchen Liu[a,b] *, Jian Kang[c]*

[a] *State Key Laboratory of Pulp and Paper Engineering, South China University of Technology, Guangzhou 510641, China.*

[b] *College of Textiles, Zhongyuan University of Technology, Zhengzhou 450007, China*

[c] *Research Institute of Chemical Defense, Beijing, 100191, China.*

Experimental section

Materials

Beta-cyclodextrin (β-CD) (98% purification), sodium periodate (NaIO4, purity>99%), gelatin (Gel, 260 bloom strength), acrylamide (AM, A8887), ammonium persulfate (APS, A9164), N,N,N',N'-tetramethylenediamine (TEMED, T7024), N,N'-methylenebis (MBAA, M7279), sodium chloride (NaCl, 99%) were purchased from Aladdin. All reagents were used as received without further purification.

Preparation of dialdehyde β-CD (O-β-CD)

β-CD (30.0 g) and sodium periodate were dissolved in 200 mL of deionized water. The mixture was agitated continuously in dark at 25 °C for 12 h. After that, the solution was filtered and the filtrate was precipitated by 800 mL ethanol. The precipitates were washed with ethanol/water (4/1, v/v) for five times and then lyophilization to obtain the products (O-β-CD).

Preparation of Gel/O-β-CDx/PAM ionic conductive hydrogels (DN-hydrogels)

First, the O-β-CDx (x refers to the weight percentage of gelatin, i.e., 1.5%, 2.0%, 2.5%) powders, gelatin, and fixed AM monomer at 20.0 wt%, NaCl (0, i.e., 5.0 wt% relative to the total weight of solvent) were dissolved in deionized water at 90 °C with a stirring. Successively, pipetting 50 μL of 100 mg/mL APS aqueous solution and 10 μL of TEMED into the above solution. Finally, The Gel/O-β-CDx/PAM ionic conductive hydrogels were prepared after polymerization at 70 °C for 3 h.

Fabrication of ionic conductive hydrogel strain/pressure sensors

The strain/pressure sensors were assembled with the ionic conductive hydrogels with a size of 5.0 × 1.0 × 0.3 cm3 and two copper tapes. The copper tapes acted as electrodes at both sides of this hydrogels to connect this hydrogel with output copper wires. Finally, this hydrogel was sealed with silicone oil to prevent water evaporation. For this flexible wearable strain sensor, the above assembled conductive hydrogels were used to fix onto the volunteer's elbow joint, forefinger, opisthenar, throat, cheek and forehead by using commercial tapes to sense the motions.

Characterization

The transform infrared (ATR-FTIR) spectroscopy and ultraviolet and visible (UV–vis) absorption spectra were recorded by Bruker Vertex 33 spectrometer, NETZSCH tester, and Cary 5000 spectrophotometer, respectively. The scanning electron microscopy (SEM) was carried out on a MERLIN SEM of ZEISS to

observe the surface morphologies. The transmittance was characterized by utilizing Agilent Cary60 UV–vis spectrophotometer. The X-ray diffraction (XRD) was performed using a polycrystall XRD (Rigaku SmartLab SE, Japan). The swelling behavior of the dried hydrogels was measured by recording their weight changes in phosphate buffered saline (PBS) solution (pH=7.0) over time. The swelling ratio (SR) was calculated according to the Equation (1):

$$SR = (m_i - m_0)/m_0 \quad (1)$$

Where m_0 is the weight of the dried hydrogel and m_i is the weight of the hydrogel at different time intervals.

Ultimate mechanical strength measurements were taken utilizing a tensile machine (INSTRON 5565, 500N load cell). Each sample was cut into a strip (1.0 × 4.0 cm^2) for testing and circle piece (diameter 2.0 cm) for compression testing. The conductivity of the hydrogels was measured at 25 °C and 35% relative humidity through EIS measurement. The measuring instrument was CHI660E Electrochemical workstation underwent the current ranging of 200 mA, and the frequency range from 1 Hz to 1MHz. The sample was cut into pieces 5.0 cm (width) × 5.0 cm (length) × 1.0 cm (thickness) and sandwiched by copper tapes.

The real-time resistance characteristics for BC-PDES gel sensors were recorded by DMM7501 Digital Graphical Sampling Multimeter (Keithley Instrument USA), the output voltage of this instrument for determination of resistance is 3.6 V. The conductivity was calculated according to Equation (2):

$$\rho^{-1} = L/(S \times R) = L/(S \times Z') \quad (2)$$

Where ρ is the resistivity of sample, L is the effective length of sample pieces, s means the cross-sectional area of sample, R means the resistance of sample, and Z' is the real part of impedance of sample.

The real-time resistance characteristics for all strain sensors were recorded by DMM7501 Digital Graphical Sampling Multimeter (Keithley Instrument USA), and the output voltage for determining the resistance is 3.6 V. The sample was cut into pieces 1.0 cm (width) × 5.0 cm (length) × 3.0 mm (thickness) or cut into cylinder 2.2 cm (diameter) × 1.1 cm (height) and sandwiched by copper tapes.

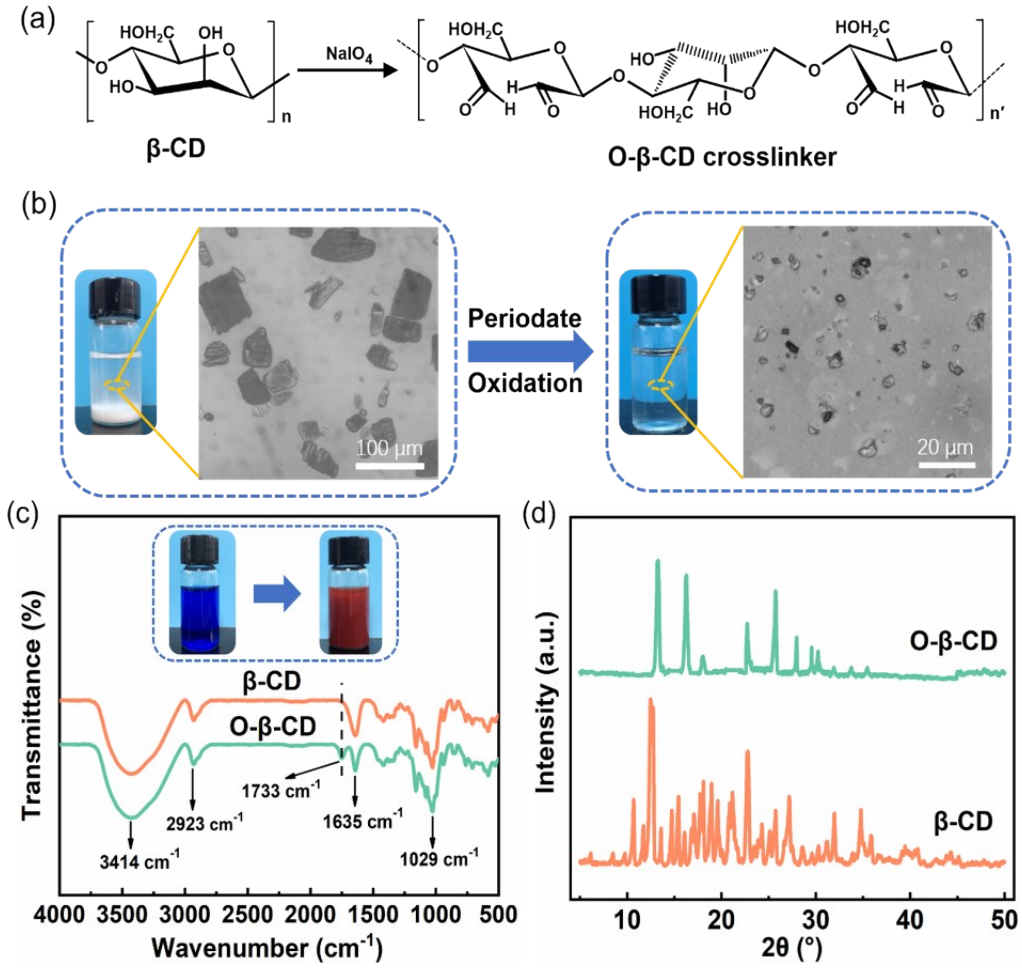

Fig. S1. (a) A schematic image of formation mechanism of O-β-CD crosslinker. (b) The aqueous solutions and micrographs of pure β-CD and O-β-CD. (c) The FT-IR spectra of β-CD and O-β-CD, the interior inset shows that the blue Flynn´reagent became red and generated precipitate after mixing the O-β-CD solution with Flynn´reagent and then heating for a few minutes. (d) XRD profiles of dried β-CD and O-β-CD.

Firstly, the preparation process and formation mechanism of O-β-CD are illustrated in Fig. S1a-b. The conversion of β-CD to O-β-CD, by oxidation of 2,3-hydroxyl of glucose to aldehyde groups, was accomplished by the procedure of periodate oxidation.[1-3] The XRD and optical microscopy were used to detect the crystal structure of β-CD and O-β-CD. Note that several peaks at 12.7° 15.5°, 17.3°, 19.8° and 20.9° were disappeared and new peaks at 22.4°, 25.9°, 28.3°, 29.6°, 30.1° (2θ) were showed in the pattern of O-β-CD (Fig. S1d).[4] Meanwhile, the micrographs observation showed that the surface of O-β-CD turned much rough and the granule size was tiny and irregular compared with β-CD (Fig. S1b).[5-7] The results indicated that periodate oxidation severely damaged the molecular structure of β-CD and changed the original crystal structure. In addition, the phenomenon that the β-CD solution precipitated quickly while the resulting O-β-CD solutions could remain stable all the time, which indicated that the aqueous solubility and dispersibility of O-β-CD was higher than that of β-CD (Fig.S1b).[4,5] For FT-IR spectra, a new peak at around 1733 cm^{-1} was observed in the spectrum of O-β-CD, and it was assigned to the C=O stretching vibration (Fig. S1c).[8,9] The result confirmed that β-CD was efficiently oxidized by $NaIO_4$, and the successful transformation of hydroxyl groups into carbonyl groups.

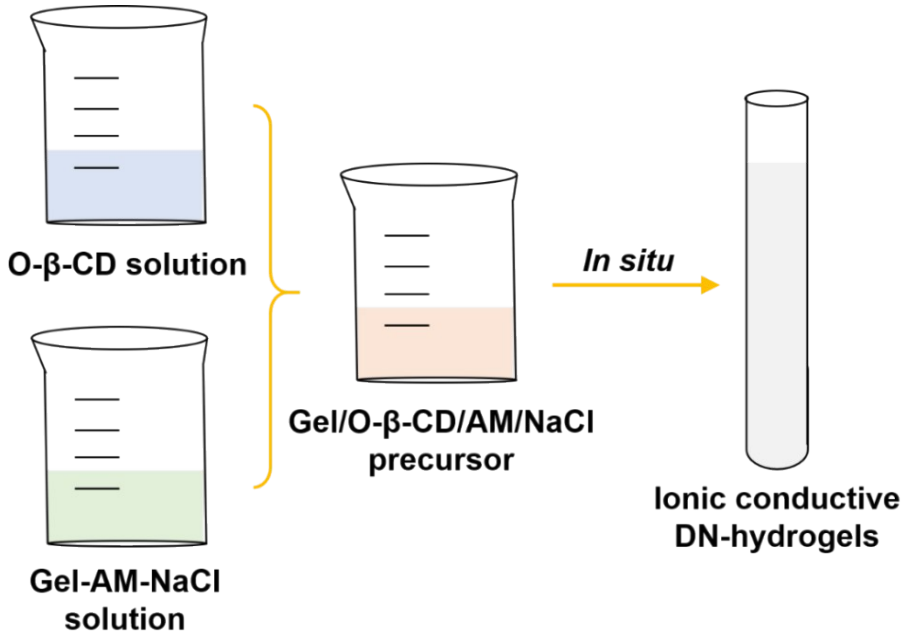

Fig. S2. Digital images of the preparation process for the ionic conductive DN-hydrogels.

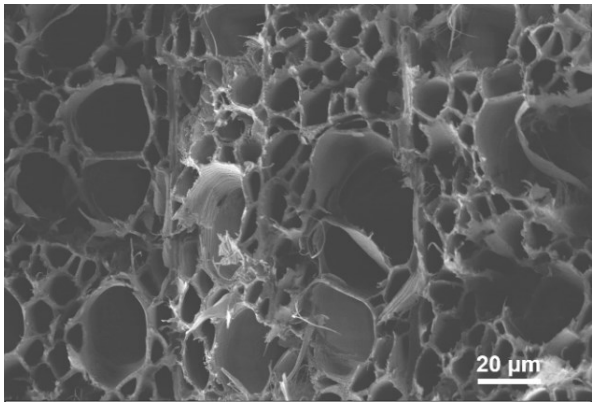

Fig. S3. SEM images of dried DN-hydrogel with O-β-$CD_{1.5\%}$ in cross-section.

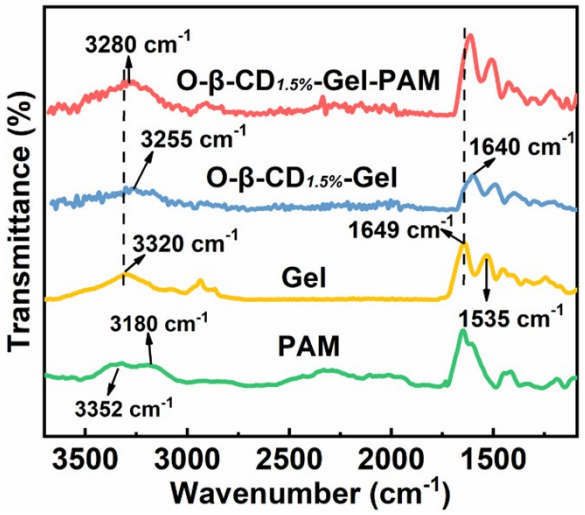

Fig. S4. ATR spectra of dried Acrylamide, Gelation, SN-hydrogel with O-β-$CD_{1.5\%}$ and DN-hydrogel with O-β-$CD_{1.5\%}$.

The characteristic O-β-CD peak at 1735 cm^{-1} completely disappeared after crosslinking with gelation. Together, the new peak at 1640 cm^{-1} of the O-β-CD/Gel, further corroborating the formation of dynamic Schiff base chemical bonds (C=N) between the amino group of Gel and the aldehyde group of O-β-CD.[10-12]

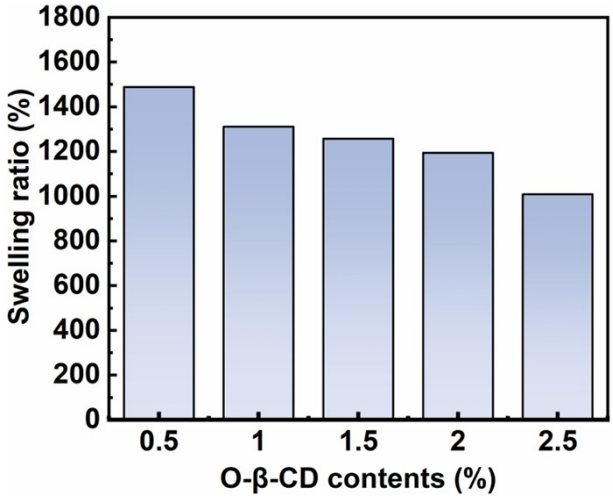

Fig. S5. The swelling ratios of the DN-hydrogels with different concentrations of O-β-CD in the PBS (pH=7) aqueous solutions at 25 ℃.

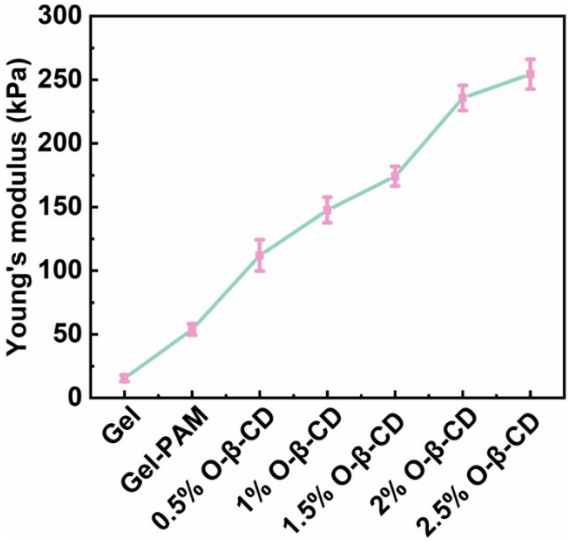

Fig. S6. Tensile stress−strain curves corresponding Young's modulus of the DN-hydrogels with different concentrations of O-β-CD.

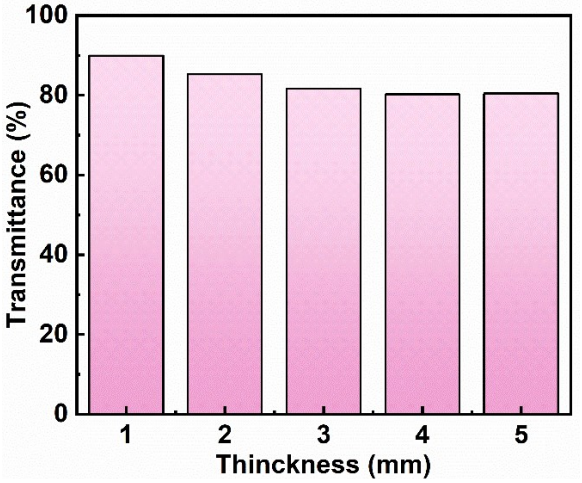

Fig. S7. Statistics of the transmittance values for different thicknesses of the DN-hydrogels with O-β-$CD_{1.5\%}$.

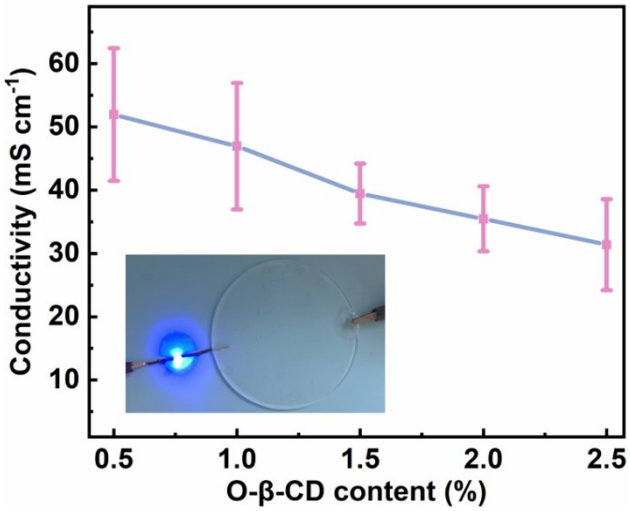

Fig. S8. The ionic conductivity of ionic conductive DN-hydrogels with different content of O-β-CD. Inset is a digital image of DN-hydrogels with O-β-$CD_{1.5\%}$.

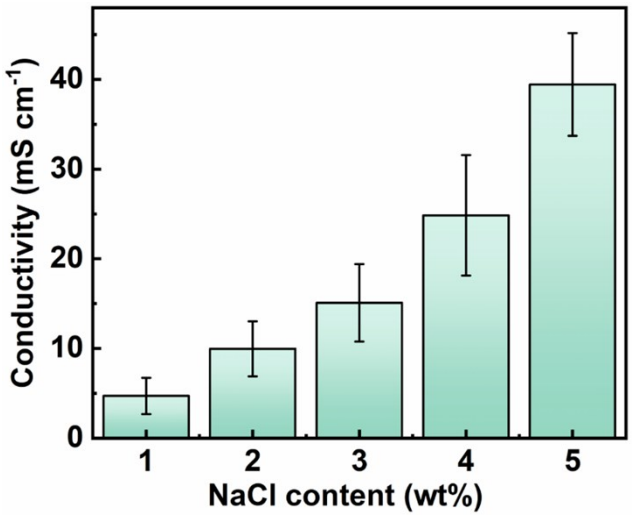

Fig. S9. Ionic conductivity of ionic conductive DN-hydrogel with O-β-$CD_{1.5\%}$ increases with increase of the NaCl content.

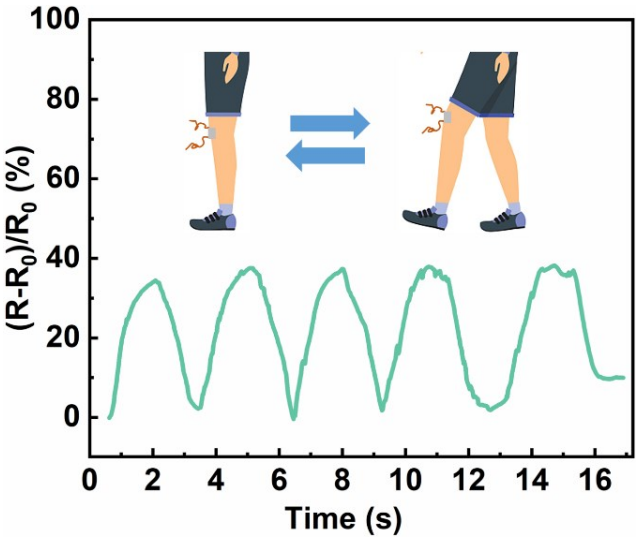

Fig. S10. Relative resistance changes vs time of the bending and releasing of knee.

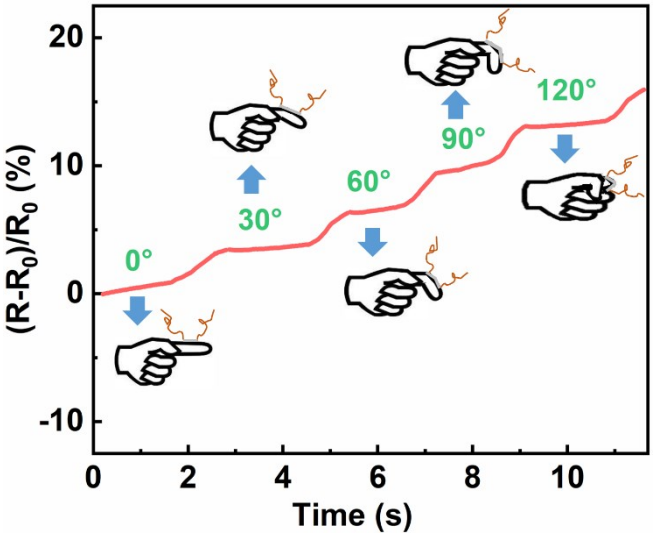

Fig. S11. Relative resistance changes versus test time for DN-hydrogel with O-β-$CD_{1.5\%}$ as sensor to detect the straightening and bending of the forefinger at different angles.

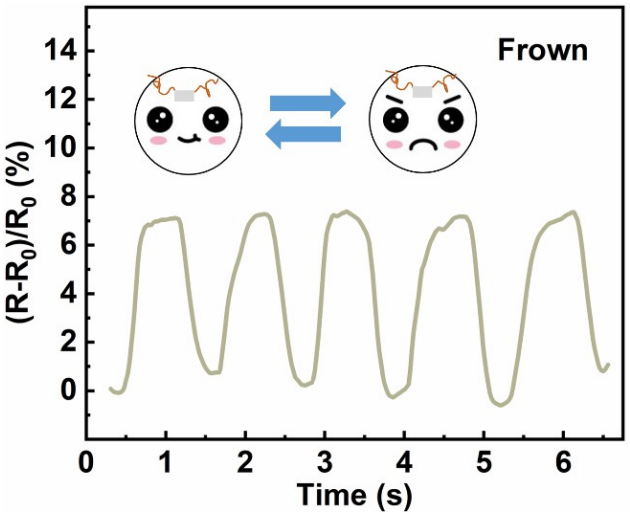

Fig. S12. Relative resistance changes vs time when sensor was attached on the brows to sense frown.

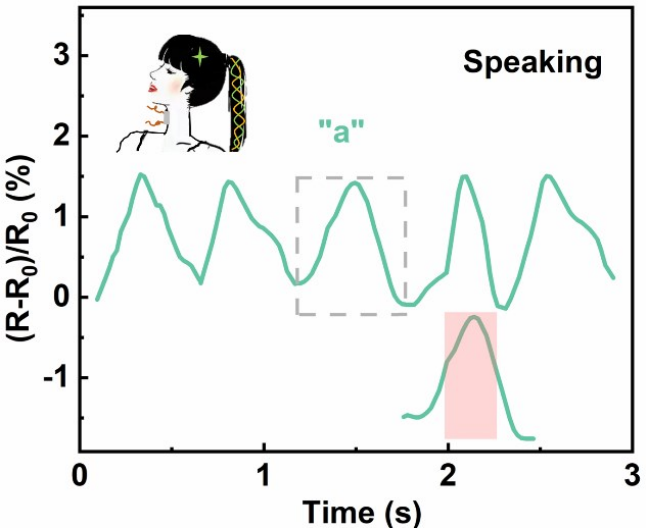

Fig. S13. The DN-hydrogel with O-β-$CD_{1.5\%}$ was attached on the throat as flexible wearable sensors for real-time monitoring different voice signals: “a”.

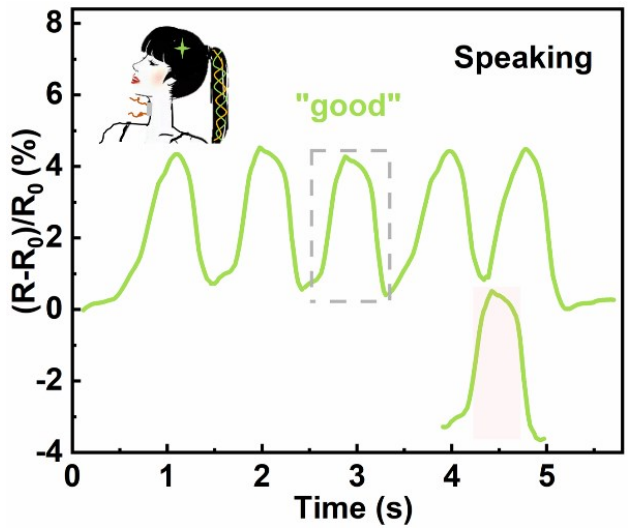

Fig. S14. The DN-hydrogel with O-β-$CD_{1.5\%}$ was attached on the throat as flexible wearable sensors for real-time monitoring different voice signals: “good”.

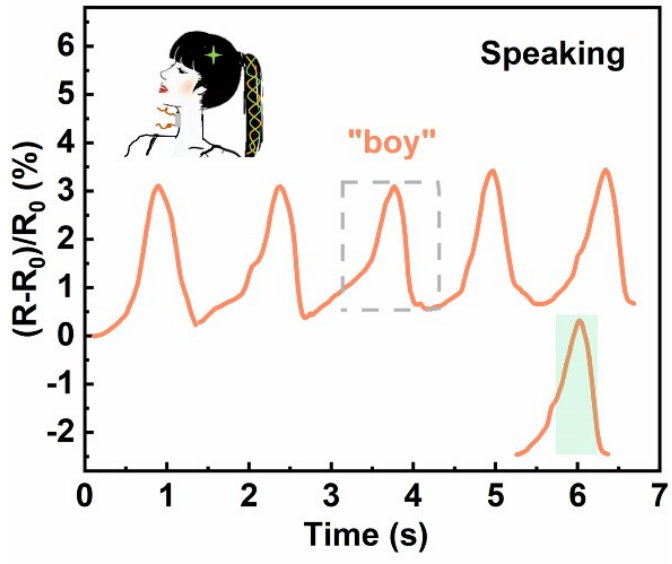

Fig. S15. The DN-hydrogel with O-β-$CD_{1.5\%}$ was attached on the throat as flexible wearable sensors for real-time monitoring different voice signals: "boy".

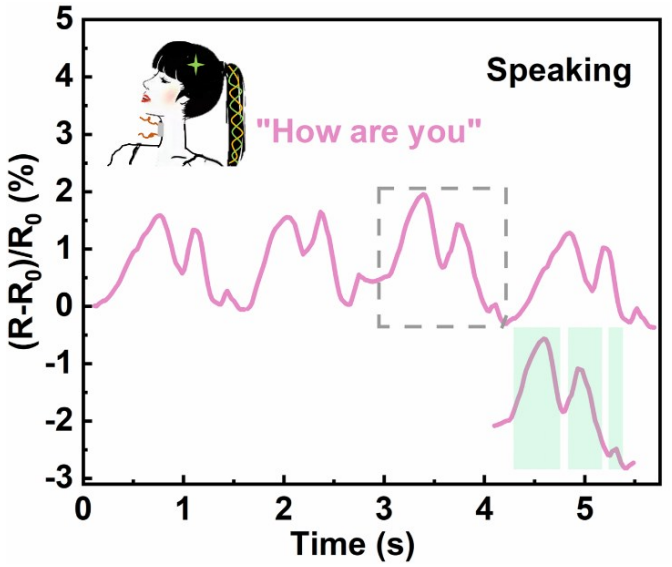

Fig. S16. The DN-hydrogel with O-β-$CD_{1.5\%}$ was attached on the throat as flexible wearable sensors for real-time monitoring different voice signals: "How are you".

Table S1. Comparison between our work and reported literatures in terms of performances.[1–16]

Materials	Compression Stress (kPa)	Stretchability (%)	Ionic conductivity (mS/cm)	Sensitivity	Transparency (%)	Ref
PVA /Sodium tetraborate /PDA	4	~500	--------	0-0.9998 (range of 0%-500% strain, nonlinear)	No	13
PAAm /PEGDA/ $MgCl_2$	＜250	＜650	--------	0-3.6 (range of 0%-200% strain, nonlinear)	＜90	14

HPC/PVA/NaCl	1.3 × 10^3 (Tensile)	975	34	0-2 (range of 0%-400% strain, nonlinear)	No	15
AMP/PAAm/ NaCl	＜70	2160	--------	0-2.37 (range of 0%-100% strain, nonlinear)	No	16
PAA/ ChCl/LA/ Fe^{3+}	152 (Tensile)	1100	2.8 × 10^{-2}	0-3.69 (range of 0%-300% strain, nonlinear)	＜89	17
Cellulose–PDA/PAM/ Fe^{3+}	＜65	92	＜0.3	--------	No	18
PDAC/PAM/ CNT	＜550	1017	1.35× 10^{-2}	--------	No	19
PAANa/ Tb^{3+}/PVA	5.5 × 10^3	＜350	30.4	--------	No	20
PAAm/ PAA/ Fe^{3+}/NaCl	1.36 × 10^3 (Tensile)	＜650	7.2	1.23-1.96 (range of 0.2%-500% strain, nonlinear)	No	21
PAA/ChCl /P(DES)	＜200 (Tensile)	150	2	0-1.5 (range of 0%-40% strain, nonlinear)	81	22
PAAM/ PAA/ Fe^{3+}/ MoS_2	1.12 × 10^3	594.6	4.6	1.5-9.06 (range of 0%-400% strain, nonlinear)	No	23
PVA/PAA/ Fe^{3+}	＜200 (Tensile)	1400	1.4	0.018 kPa^{-1} (range of 0-100kPa pressure, linear)	Translucent	24
PDA/ Talc/PAM/ KCl	＜32	～1000	--------	0-0.693 (range of 0%-1000% strain, nonlinear)	Translucent	25
PVA/PAA/ Fe^{3+}/CNT/PEDOT:PSS/EG	28.33 (Tensile)	550	--------	0.66-1.66 (range of 0%-100% strain, nonlinear)	No	26
Gelatin/ ChCl/EG	＜70 (Tensile)	300	25	0.5 (range of 0%-125% strain, linear)	Yes	27
PVAA/PAM/ Fe^{3+}	＜400 (Tensile)	700	32	0.2	90	28
Gelatin/ O-β-CD/ PAM/NaCl	682	＞1200	53.3	4.58 (range of 0%-1200% strain, linear); 0.56 kPa^{-1} (range of 0 kPa～250 kPa, pressure, linear).	89	This Work

References

[1] S. Zhang, X. Wang, Y. Zhang, Journal of Polymer Research, 2010, 17, 439.

[2] W. Ding, J. Zhou, Y. Zeng, Carbo. Polym, 2017, 157, 1650.

[3] M. Kobayashi, T. Urayama, I. Suzawa, S. Takagi, Agric. Biol. Chem, 1988, 52, 2695.

[4] Y. Zhou, Y. Ye, W. Zhang, Carbo. Polym, 2016,154, 13.

[5] J. L. Wang, Z. D. Yao, C. W. Monroe, J. Yang, Adv. Funct. Mater, 2013, 23, 1194.

[6] Y. X. Ye, H. Ren, S. Zhu, Carbo. Polym, 2017, 1, 97.

[7] H. Ren, Y. Lyu, X. Li, Food Research International, 2018, 111, 237.

[8] J. Song, H. Kang, C. Lee, ACS Appl. Mater. Interfaces, 2012, 4, 460.

[9] N. L. Vanier, E. D. R. Zavareze, V. Z. Pinto, Food Chemistry, 2012, 131, 1255.

[10] U. Kim, Y. R. Lee, T. H. Kang, Carbo. Polym, 2017, 163, 34.

[11] L. Liu, H. Wen, Z. Rao, International Journal of Biological Macromolecules Structure Function & Interactions, 2018, 108, 376.

[12] U. J. Kim, Y. R. Lee, T. H. Kang, J. W. Choi, Carbo. Polym, 2017, 163, 34.

[13] S. Liu, R. Zheng and S. Chen, J. Mater. Chem. C, 2018, 6, 4183.

[14] X. Yin, Y. Zhang, X. Cai, Mater. Horiz., 2019, 6, 767.

[15] Y. Zhou, C. Wan and Y. Yang, Adv. Funct. Mater, 2019,29, 1806220.

[16] Q. Zhang, X. Liu and X. Ren, Chemistry of Materials, 2019, 31, 5881.

[17] C. Dang, M. Wang and J. Yu, Adv. Funct. Mater, 2019, 29, 1902467.

[18] L. Li, F. Lu and C. Wang, J. Mater. Chem. A, 2018, 6, 24468.

[19] C. Pan, J. Wang and X. Ji, J. Mater. Chem. C, 2020, 8, 1933.

[20] J. Lai, H. Zhou and M. Wang, J. Mater. Chem. C, 2018, 6, 13316.

[21] S. Li, H. Pan and Y. Wang, J. Mater. Chem. A, 2020, 8, 3667.

[22] R. Li, G. Chen and M. He, J. Mater. Chem. C, 2017, 5, 8475.

[23] J. Wang, Y. Liu and S. Wang, Colloids and Surfaces A: Physicochemical and Engineering Aspects, 2020, 610, 125692.

[24] S. H. Shin, W. Lee and S. M. Kim, Chemical Engineering Journal, 2019, 371, 452.

[25] X. Jing, H. Mi and Y. Lin, ACS Appl. Mater. Interfaces, 2018, 10, 20897.

[26] X. Dong, G. Ge and W. Yuan, J. Mater. Chem. A, 2019, 7, 5949.

[27] H. Qin, R. E. Owyeung and S. R. Sonkusale, J. Mater. Chem. C, 2019, 7, 601.

[28] J. Tie, L. Rong and H. Liu, Polym. Chem, 2020,11, 1327.